ELSEVIER

European Journal of Cancer 40 (2004) 890–898

European Journal of Cancer

www.ejconline.com

A potential role for imaging technology in anticancer efficacy evaluations

M.G. Hollingshead[a,*], C.A. Bonomi[b], S.D. Borgel[b], J.P. Carter[b], R. Shoemaker[a], G. Melillo[b], E.A. Sausville[a]

[a]*Developmental Therapeutics Program, Division of Cancer Diagnosis and Treatment, National Cancer Institute, Bethesda, MD 20892, USA*
[b]*SAIC-Frederick Inc., PO Box B, Frederick, MD 21702, USA*

Received 4 November 2003; received in revised form 27 November 2003; accepted 18 December 2003

Abstract

The introduction of imaging methods suitable for rodents offers opportunities for new anticancer efficacy models. Traditional models do not provide the level of sensitivity afforded by these precise and quantitative techniques. Bioluminescent endpoints, now feasible because of sensitive charge-coupled device cameras, can be non-invasively detected in live animals. Currently, the most common luminescence endpoint is firefly luciferase, which, in the presence of O_2 and ATP, catalyses the cleavage of the substrate luciferin and results in the emission of a photon of light. *In vivo* implantation of tumour cells transfected with the luciferase gene allows sequential monitoring of tumour growth within the viscera by measuring these photon signals. Furthermore, tumour cell lines containing the luciferase gene transcribed from an inducible promoter offer opportunities to study molecular-target modulation without the need for *ex vivo* evaluations of serial tumour samples. In conjunction with this, transgenic mice bearing a luciferase reporter mechanism can be used to monitor the tumour microenvironment as well as to signal when transforming events occur. This technology has the potential to reshape the efficacy evaluations and drug-testing algorithms of the future.
Published by Elsevier Ltd.

Keywords: *In vivo* imaging; Bioluminescence; Luciferase; Cancer efficacy studies

1. Introduction

The development of new therapies for neoplastic disease involves a series of steps designed to improve the probability of a positive outcome when the agent is taken into human clinical trials. An important component of this process is to determine the therapeutic potential in animal models of neoplastic disease. Assessing the activity of proposed new therapies in rodent models has been a critical component of the National Cancer Institute drug-development algorithm for over 45 years. These *in vivo* efficacy evaluations have historically relied upon our capacity to monitor tumour growth by one of two methods: the direct observation of superficially growing tumours or the monitoring of alterations in the lifespan of animals [1]. For models of metastatic and disseminated disease, morbidity/mortality has often served as a marker for tumour growth. Refinement of these studies is achieved by detailed pathological and histological evaluations of tumour distribution within the experimental animals, including the use of metastasis counts in the lungs and organ weights in the abdominal viscera [2,3]. While these systems have served us well in advancing potential therapies to clinical trial, they are limited in several regards. First, it is impossible to detect small changes in tumour mass when only the gross tumour dimensions serve as the endpoint. Secondly, to detect visceral tumours the experimental animal must be killed and so progressive monitoring of the growth of a visceral tumour cannot be readily achieved. Thirdly, to measure changes in molecular targets requires the collection of tumour samples that are subsequently subjected to *in vitro* analytic methods for the quantitation of protein or genetic changes [4], making assessments of multiple time points within a single host difficult if not impossible [4,5]. Finally, these models cannot easily address many of the issues associated with defining micrometastatic disease.

* Corresponding author. Tel.: +1-301-846-5608; fax: +1-301-846-6183.
E-mail address: hollingm@mail.nih.gov (M.G. Hollingshead).

0959-8049/$ - see front matter Published by Elsevier Ltd.
doi:10.1016/j.ejca.2003.12.018

The advent of imaging methods applicable to rodents offers the opportunity to circumvent many of these limitations. These techniques allow repeated images from tumour-bearing animals without the need for serial killing. A variety of these techniques have been extensively reviewed elsewhere [6–14]. These techniques can be separated, based upon the endpoint being imaged, into two broad categories, extrinsic and intrinsic. For imaging of extrinsic features, any tumour can be imaged whether it is of exogenous (e.g. transplanted, chemically induced) or endogenous origin (e.g. transgenic mouse tumour models), as the endpoint results from structural or biological changes in the soft tissues. Magnetic resonance imaging, which provides three-dimensional structural imaging that can be augmented with contrast agents [6,7,15,16], is one example of a tumour-independent, tissue-dependent imaging technique. A second extrinsic approach is X-ray computed tomography (CT), now applicable to rodent studies through commercially available micro-CT scanners (GE Medical Systems, Ontario, Canada; ImTek, Inc., Knoxville, TN). The micro-CT allows high-resolution imaging (50 μm and below) of soft tissue structures and can be used in conjunction with contrast media [5,6,17]. A third technique, positron-emission tomography (PET), now available in a micro-PET format (Concorde Microsystems, Inc. Knoxville, TN, USA) [18], provides opportunities to image biochemical processes occurring in small rodent species using a variety of probes that target molecular, enzymatic or metabolic endpoints [19–21]. These methods are being very actively researched, at least in part because new probes, improved sensitivities and expanding applications can be rapidly translated to human use as the basic techniques are already an important part of human clinical investigations. Unfortunately, their use in preclinical studies of antitumour efficacy is limited by the expense of the equipment, the protracted time required for image collection and the complex nature of the data analysis. For operations in which relatively large numbers of compounds are evaluated, access to the imaging equipment can be a limiting feature since only one animal can be imaged at a time.

While extrinsic imaging is valuable in many aspects, the use of tumours with intrinsic characteristics amenable to optical imaging offers a range of features that can readily serve drug development. Two endpoints currently available for *in vivo* optical imaging are fluorescence and bioluminescence. The primary difference between them is the requirement for external light at the appropriate excitation wavelength to induce fluorescence while bioluminescence is independent of external light. Both fluorescence and bioluminescence have been broadly applied to *in vitro* assays for many years but the advent of extremely sensitive, charge-coupled device cameras [12,22] has provided opportunities for application to *in vivo* studies [23–26].

The most commonly known fluorescence markers are probably those associated with immunohistochemistry, e.g. fluorescein and rhodamine. There is, however, a wide array of fluorescent molecules currently under development for evaluating tumour growth *in vivo* [10,14,27–33]. These include molecules that are specifically targeted to tumour cells via antibodies [14], molecules that fluoresce following metabolic cleavage within tumour cells [29,30] and endogenously synthesised fluorescent proteins in genetically altered tumour cells [32,33]. The development of fluoroprobes that are metabolically activated by tumour cells offers the opportunity to monitor tumour growth using fluorescence endpoints both in experimental animals and, ultimately, in the human clinical setting. For example, Mahmood and colleagues [27] describe the use of a cleavable fluorochrome, PCG-Cy5.5, that is activated following intratumoral cleavage by cathepsin B and they have demonstrated its applicability to monitoring tumour growth in rodents. As an alternative to exogenously administered fluorochromes, tumour cells can be genetically altered to express fluorescent proteins. Perhaps the best known of these is the green fluorescent protein originally isolated from the jellyfish *Aequorea victoria* [5]. A range of other fluorescent proteins has been isolated and may provide alternative, more sensitive *in vivo* reporters for tumour cell growth [5]. The use of tumour cells constitutively expressing one of these fluorescent proteins allows tumour growth to be monitored *in vivo*, provided the tumour's depth does not preclude the detection of the fluorescence [5,33].

The second optical imaging endpoint, bioluminescence, is the production of visible light during an enzymatic reaction. The responsible enzymes, generically named luciferases, act on chemical substrates commonly referred to as luciferins [5]. A variety of organisms produce luciferases, including species of bacteria, marine organisms and insects [5]. The most common enzyme-substrate pairing used for cell labelling is the luciferase from the male firefly, *Photinus pyralis*. The gene for firefly luciferase was isolated and subsequently expressed in mammalian cells by de Wet and colleagues [34,35]. The gene is commercially available in various plasmid constructs, which makes the method broadly available to the research community. The enzyme catalyses the reaction [ATP + firefly luciferin + O_2 → AMP + oxyluciferin + PPi + light (560 nm)] in the presence of Mg^{2+} [24]. Introducing the firefly luciferase gene into mammalian cells provides a bioluminescent marker that is visualised when luciferin is added. This approach to tumour imaging for efficacy evaluations has a variety of advantages. These include short imaging times (< 1 min), the ability to image many animals simultaneously, the commercial availability of equipment and analysis software (Xenogen Corp., Alameda, CA, USA), the greater sensitivity compared to fluores-

cence since excitation light is not required, the ability to image visceral tumours, the capacity to construct luciferase reporters operating from specific promoters, the absence of background light emission from rodent tissues, the short half-life of the enzyme in mammalian tissues (about 3 h) and the non-toxic nature of the luciferin [12,24,36–42]. For these reasons we have opted to investigate firefly luciferase as a bioluminescent marker for *in vivo* tumour studies.

2. Materials and methods

2.1. Cell lines

U251-pGL3 and U251-HRE, two cell lines prepared by Melillo and colleagues from the human glioma U251 [43], were used in all studies reported here. U251-pGL3 is stably transfected with a constitutively producing luciferase gene. U251-HRE cells have a luciferase gene operating from an inducible promoter. The promoter is hypoxia-responsive so that luciferase activity 'reports' when the cells are exposed to hypoxic conditions. Both cell lines were cultured *in vitro* in RPMI-1640 (Quality Biologicals, Gaithersburg, MD, USA) containing 10% fetal calf serum (Hyclone, Logan, UT, USA), 1% L-glutamine (Invitrogen Life Technologies, Carlsbad, CA) and 100 μg/ml G418 (Invitrogen). Cells were maintained by serial *in vitro* passage.

2.2. Animal studies

All studies were conducted in an AAALAC accredited facility in compliance with the PHS *Guidelines for the Use of Animals in Research*. The majority of studies were conducted in athymic nude (nu/nu NCr) mice, with severe combined immunodeficient mice used for comparative purposes in a few experiments. All mice, obtained from the animal production facility at NCI-Frederick, were given autoclaved feed and hyperchlorinated water ad libitum. Tumour cell inoculations were performed when the mice were 6–8 weeks of age. Luciferase activity was imaged 15 min following intraperitoneal (i.p) administration of 150 mg/kg luciferin (Xenogen Corp., Alameda, CA, USA).

2.3. Imaging hardware and software

All bioluminescent data were collected and analysed with a Xenogen IVIS® system. This is a user-friendly system that automates many of the steps in data collection and storage. The operator sets the imaging variables and the system collects a photographic and bioluminescent image of the sample. The bioluminescence data are visually presented as a colour overlay on the photographic image. The Xenogen IVIS® software allows quantitative measurements of bioluminescence within any region of interest (ROI) selected by the operator through placement of boundaries around the desired measurement area(s). The bioluminescence is quantified and reported as photons/s per ROI. Data are stored on a local computer. The system is equipped with an isoflurane gas anaesthetic delivery system that scavenges waste gases to protect the operator. The imaging surface is heated (37 °C) to maintain homeostasis in the animal during anaesthesia and imaging. This allows the mice to be anaesthetised for protracted periods of time if serial sampling is desired. Up to 10 mice can be imaged simultaneously if injectable anaesthetics are used. For inhalation anaesthesia there are five delivery ports, so five mice can be imaged simultaneously during isoflurane anaesthesia.

3. Results

The initial effort was to define the level of detection possible with the U251-pGL3 tumour cells. The U251-pGL3 cells were plated into a 96-well microtitre plate, starting at 1×10^4 cells/well and continuing with serial 2-fold dilutions to a theoretical 19.6 cells/well. The cells were imaged 3 h after plating by adding firefly luciferin (Xenogen) to a final concentration of 150 μg/ml. Fifteen minutes after luciferin addition, the plates were imaged for 3 min. Using a 96-well grid ROI pattern, the luminescence from each well was quantitated. The average and S.D. for luminescence readings from each cell density ($n=8$/density) were plotted as shown in Fig. 1. Controls included eight media control wells containing medium to which luciferin was added without cells present and eight cell control wells containing cells and medium to which no luciferin was added. The values of these controls define the minimum detection level for the assay. The photon/s readings for the 20 cells/well samples were statistically significantly different from both control values, implying that as few as 20 cells can be detected with this endpoint. This sensitivity suggested that the cells should be detected following *in vivo* administration. Thus, serial dilutions of the U251-pGL3 cells were injected by each of four routes: subcutaneous (s.c), intrarenal (i.r), intracranial (i.c) and intravenous (i.v). The mice were imaged 3 h after tumour inoculation. As seen in Fig. 2, it was possible to detect tumour in all four implant sites, with the lungs being the primary organ in which the i.v-administered cells were localised. The level of detection in this assay was 1×10^5 cells s.c, 5×10^4 cells i.c, 5×10^3 cells i.r and 5×10^5 cells i.v. The question then is how much more sensitive is the bioluminescent endpoint than the classical tumour measurement endpoint? To answer this, a series of mice were implanted s.c with serial dilutions of a clone of U251-pGL3 selected for high endogenous expression of

luciferase activity (n = four mice/density). The mice were monitored 2–3 times each week for the presence of measurable tumour masses and for the presence of bioluminescence at the tumour implant site. As shown in Table 1, the bioluminescence endpoint was many fold more sensitive than the classical method for tumour measurement. For each animal and time point at which there was a measurable tumour the photons/s per mg of tumour was calculated. The average and median values calculated from all the data points irrespective of the tumour volume were 1.9×10^6 and 1.7×10^6 photons/s per mg of tumour, respectively. It is worth noting that the early signal measured on day 2 decreases steadily for about 2 weeks, after which there is a steady increase in signal.

A preliminary evaluation of the value of the luminescence endpoint for anticancer drug evaluations was conducted with the cloned line of U251-pGL3 cells. For this, 1×10^5 cells/0.1 ml were injected s.c into 20 mice. On day 6 after the tumour injection the mice were randomised into a vehicle- (n = 10) and a drug treated group (n = 10). The vehicle controls received three i.p doses of 2% ethanol in saline given on an every fourth day (Q4D×3) schedule. The treated group received 12.5

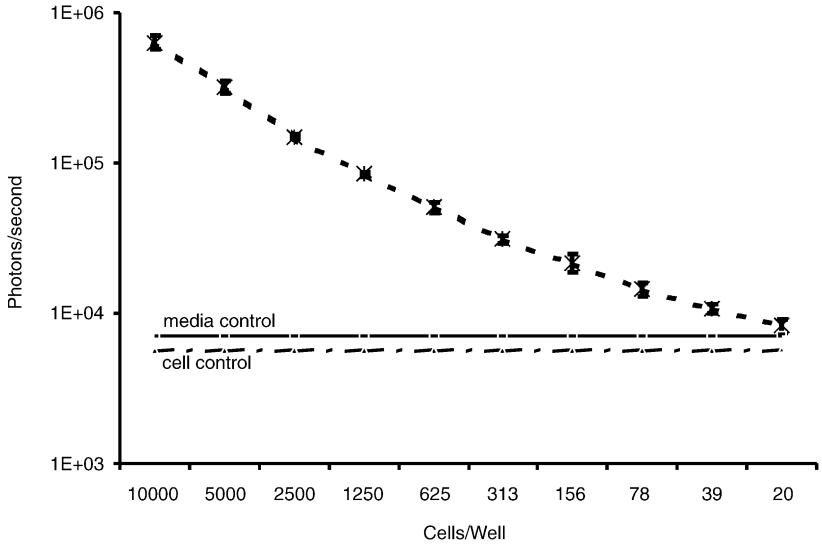

Fig. 1. U251-pGL3 cells were plated in serial 2-fold dilutions into a 96-well plate with high density at 1×10^4 cells/well. 3 h after plating each well was adjusted to a final concentration of 150 μg of firefly luciferin/ml of medium. Bioluminescence was measured 15 min later. Photon emissions were collected for 3 min. The average photons/s for each cell density are plotted (n = 8/dilution). The media control is the average photons/s for eight wells containing media and luciferin but no cells. The cell control is the average photons/s for eight wells containing cells without luciferin.

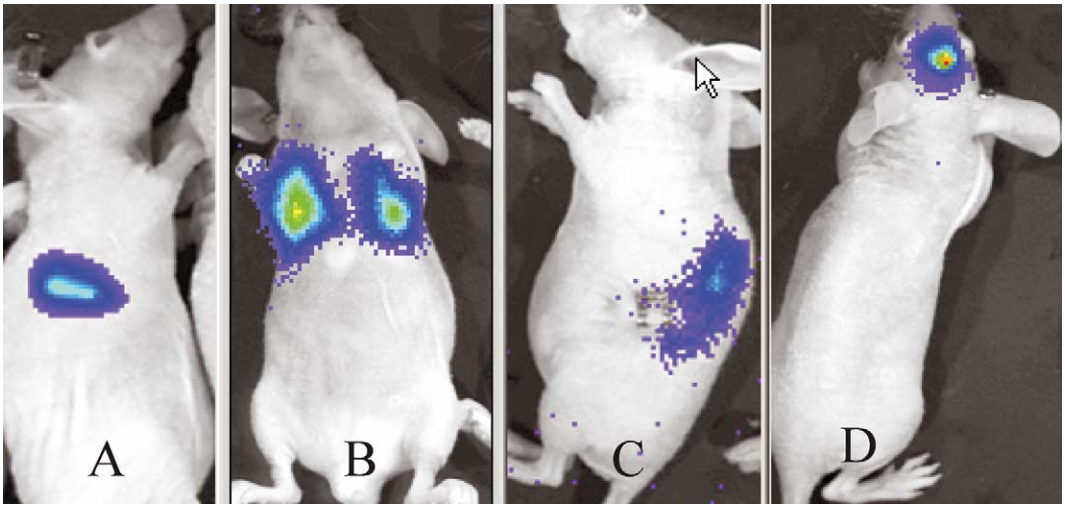

Fig. 2. Mice were injected with U251-pGL3 cells and imaged 3 h later under ketamine/xylazine anaesthesia. The mice received 150 mg/kg firefly luciferin by intraperitoneal injection 15 min before imaging. The Xenogen software provides visual images of bioluminescence detection using a coloured overlay on a photographic image taken immediately before luminescence measurements. The areas shown in colour represent the regions of bioluminescence detection. A: cells administered subcutaneously; B: cells administered intravenously; C: cells administered intrarenally; D cells administered intracerebrally.

Table 1
Median tumour weights and average luminescence values of U251-pGL3 inoculated subcutaneously into mice at varied cell densities[c]

Inoculum	Day 2	Day 7	Day 14	Day 21	Day 35	Day 49	Day 63
Average bioluminescence (photons/s $\times 10^6$)							
1×10^7 cells	427	253	152	136	279	1360	1630
5×10^6 cells	163	87	37	38	172	289	1370
1×10^6 cells	186	50	20	21	118	359	897
5×10^5 cells	28	9.6	6.7	8.3	9.7	81	520
1×10^5 cells	20	7.8	8.1	6.7	15	57	132
Median tumour weights (mg)[a]							
1×10^7 cells	0	69	+[b]	63	107	387	815
5×10^6 cells	0	+	+	+	92	288	1030
1×10^6 cells	0	+	+	+	+	184	747
5×10^5 cells	0	0	0	0	+	+	131
1×10^5 cells	0	0	0	0	+	+	86

[a] Tumour weights were calculated from bidimensional tumour measurements using the formula: [Length$\times$(width^2)]/2 = tumour weight (mg)].
[b] Palpable but too small to measure accurately ($<$63 mg or $<(5\times5)$ mm tumour).
[c] NA: not applicable—cannot divide by a tumour weight of 0 mg.

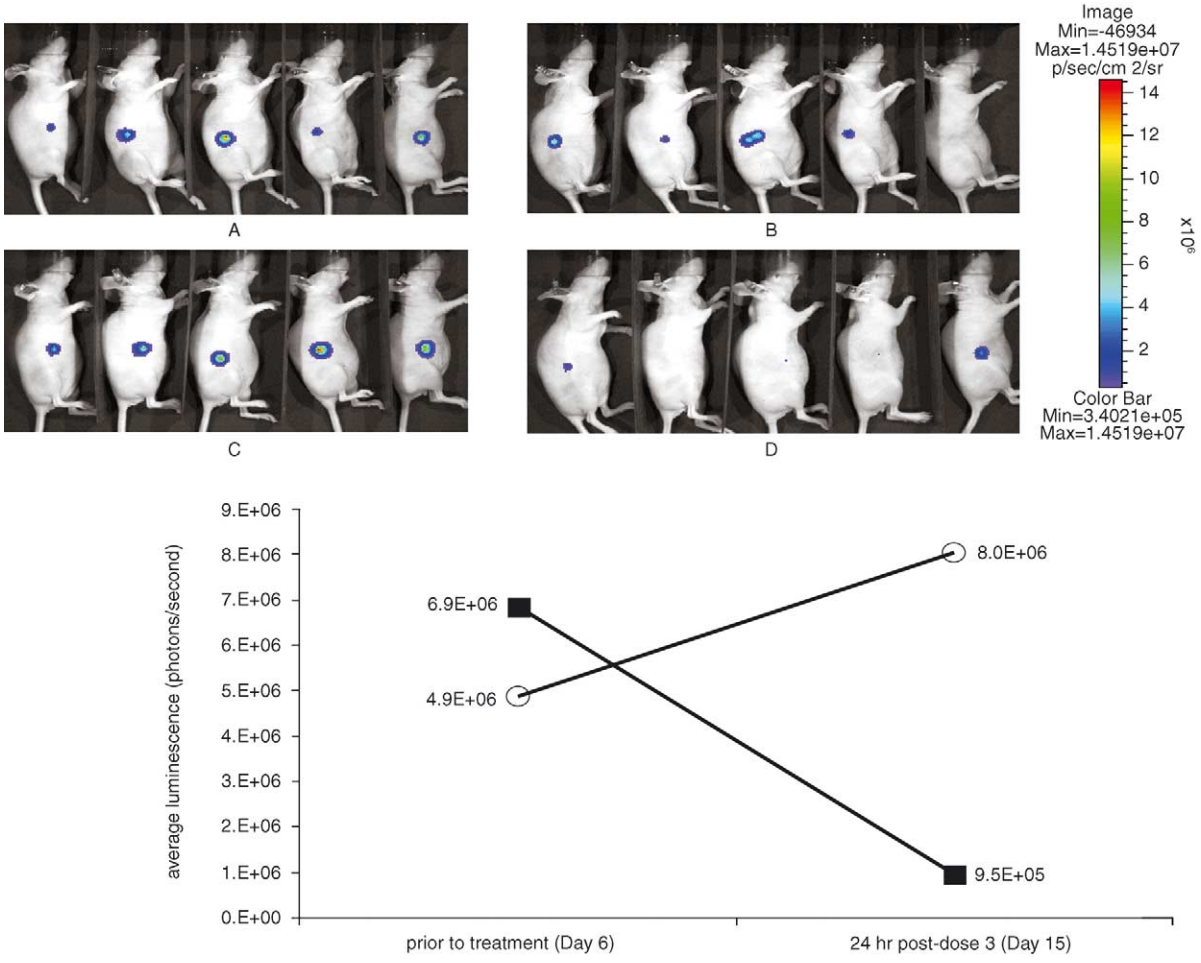

Fig. 3. 20 mice were injected subcutaneously with 1×10^5 clonal U251-pGL3 cells. On day 6 the mice were randomised to a vehicle control or 12.5 mg BCNU/kg treatment group ($n=10$/group). Treatments were administered intraperitoneally on a Q4D$\times$3 schedule. The mice were imaged just before the first treatment and 24 h after the last treatment. The luminescence intensity was normalised for all four images as shown by the colour bar to the right. (A) Vehicle control before treatment; (B) BCNU-treated group before treatment; (C) vehicle control 24 h after the third treatment; (D) BCNU-treated group 24 h after the third treatment. Five representative mice/group are shown in (A-D). The median luminescences for the vehicle controls (open circles) and the BCNU treated (solid squares) are plotted as photons/s in (E) ($n=10$ mice/group).

mg/kg BCNU (NSC 409962) on the same schedule. The mice were imaged immediately before the first dose and 24 h after the third dose. As seen in Fig. 3, there was a pronounced decrease in luminescence in the BCNU-treated group (Fig. 3B, pretreatment; Fig. 3D, post-treatment) while the control group had an increase in luminescence during the same observation period (Fig. 3A, pre-treatment; Fig. 3C, post-treatment). The average luminescences are presented graphically in Fig. 3(E). During the entire observation period, no visible or palpable tumour was detected in any of the 20 mice.

An obvious application for bioluminescence within our programme is as the endpoint for the hollow-fibre assay. The first question was whether luminescence could be detected through the wall of the hollow fibres. The U251-pGL3 cells were inoculated into hollow fibres at 1×10^5 cells/fibre as described previously [44]. The fibres were placed into 25-mm Petri dishes and incubated for 24 h at 37 °C in a humidified, 5% CO_2 atmosphere. Fifteen minutes before imaging, firefly luciferin was added to the media at a final concentration of 150 μg/ml. The fibres were imaged for 1 min and bioluminescence was readily detected through the wall of the fibre, suggesting that *in vivo* applications were feasible. Hollow fibres, inoculated with U251-pGL3 at 1×10^5 cells/fibre, were implanted into athymic mice; 3 h later the mice were anaesthetised, injected with 150 mg/kg firefly luciferin i.p and imaged every 2 min for 98 min. A representative mouse and its luminescence pattern are presented in Fig. 4 along with a graph of the average and median bioluminescences of the hollow-fibre implant site ($n=3$ mice). Initial detection of luminescence occurred between 6 and 8 min after luciferin administration. Bioluminescence continued to rise for approximately 60 min at which time it achieved a plateau that continued for the duration of the imaging period.

The preceding studies demonstrated the feasibility of using tumour cells constitutively expressing luciferase for xenograft and hollow-fibre models. The next question was whether the U251-HRE tumour cells with their inducible promoter respond as expected when implanted into mice. Mice were implanted with 1×10^7 tumour cells s.c and tumour dimensions as well as luciferase activity were monitored. As seen *in vitro*, the cell line did produce luciferase; however, unlike the U251-pGL3 cells, luciferase activity did not increase during the early

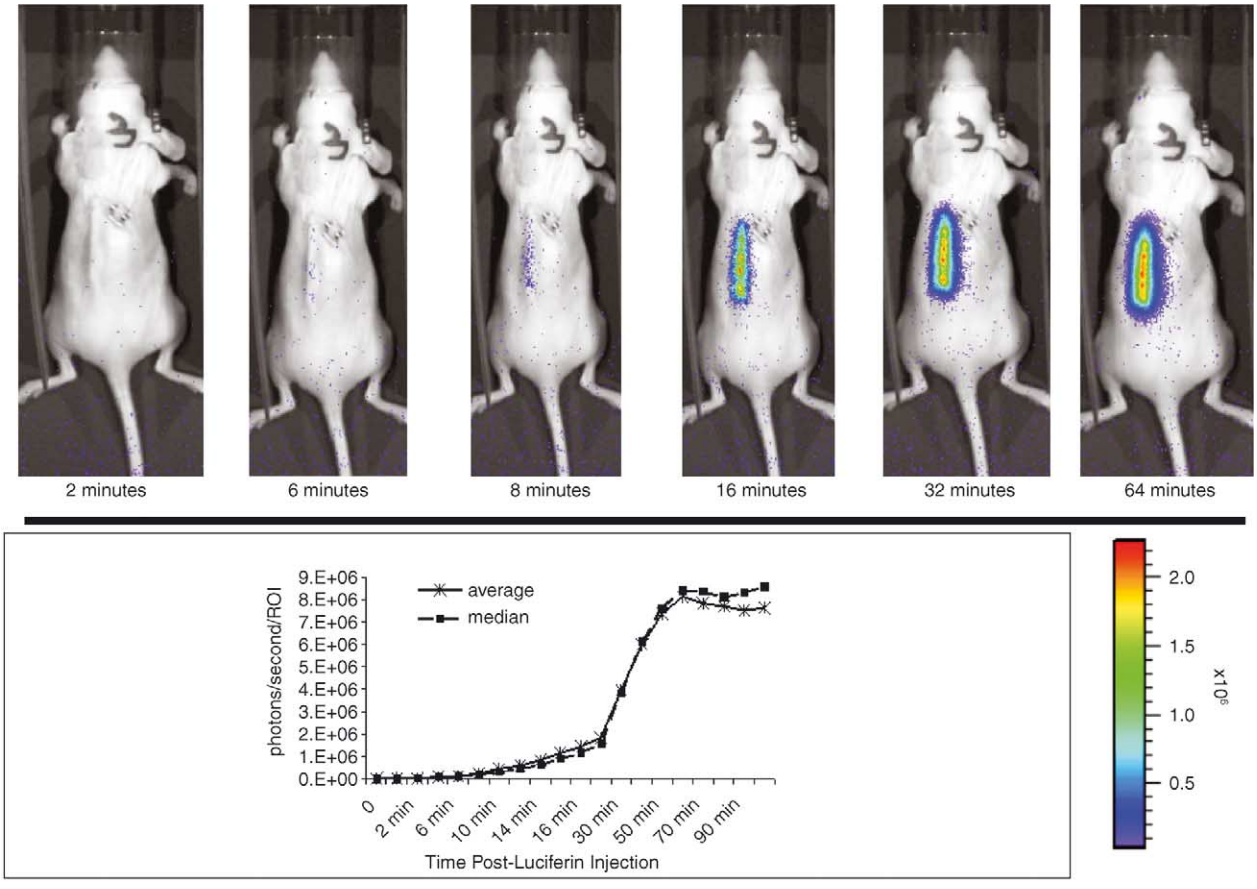

Fig. 4. Representative mouse implanted with a single fibre containing U251-pGL3 cells and imaged for 98 min starting 3 h after fibre implantation. As can be seen from the mouse, detection of luminescence becomes possible 6–8 min after injection with luciferin. The luminescence continues to increase for approximately 60 min, at which the activity reaches a plateau and remains detectable for at least 98 min. $n=5$/time point for the graph.

phase of tumour growth. Rather, it began to increase markedly once the tumours had reached 300–500 mg in size. At a median tumour weight of 500 mg the average luminescence was 5000 photons/s per mg of tumour. In contrast, the U251-pGL3 with constitutive luciferase activity produced in excess of 1.2×10^6 photons/s per mg at a median weight of 500 mg. This represents a 250-fold difference between the bioluminescence of the U251-pGL3 cells and the U251-HRE cells at a comparable tumour weight. This finding is consistent with the known hypoxic character of tumours during growth and suggests this cell line could serve as an *in vivo* model for hypoxic responses in tumour cells.

Finally, transgenic mice expressing luciferase from inducible promoters are another application for which bioluminescence imaging is valuable for drug discovery and development. These promoters may be responsive to exogenous factors or they may induce luciferase expression when the animal undergoes neoplastic transformation. We are in the early stages of developing a transgenic model in which luciferase expression is induced when the tissues become hypoxic. It is anticipated that these mice will express luciferase when transplanted tumours become hypoxic. This will provide a way of monitoring the microenvironment of the tumour rather than the tumour cells themselves. While we do not yet have data from tumour-implanted mice, we do have demonstrable evidence that the founder mice express luciferase. Future studies should reveal the biological characteristics of these mice and their potential utility.

4. Conclusions

Bioluminescence offers an opportunity to develop rodent models for efficacy evaluations that are more sensitive, more specific and of shorter duration than those traditionally used. In addition, the use of inducible promoter systems provides a possibility of understanding the mechanisms of action for new drugs without the need for time-consuming and often expensive *ex vivo* analyses of tissue samples. We have found the bioluminescent endpoint to be sensitive, as reported by others [36]. In fact, this method offers the opportunity of conducting an entire efficacy evaluation in the time historically required for tumours to stage to a measurable starting point. The detection of luminescence in the absence of a palpable tumour is a significant improvement in our capacity to detect antitumour activity; this may be particularly relevant for developing therapies to treat minimal residual or micrometastatic disease. Furthermore, since the tumour does not have to achieve a large mass, it is possible to implant multiple tumours on a single mouse, provided the luminescence from one tumour is blocked to prevent interference with data collection from the other tumours. This technique allows more data to be generated with fewer mice, less drug and lower housing requirements.

The enzyme reaction catalysed by luciferase requires oxygen and ATP. The presence of bioluminescence in tumours confirms there is oxygen present in the tumour in spite of the common view that tumours are hypoxic. The capacity of cells within hollow fibres to support bioluminescence demonstrates there is oxygenation of the contents of the fibre in spite of the lack of vascularisation. Furthermore, the rapidity with which luminescence occurs in s.c fibres following i.p administration of the substrate demonstrates the speed with which solutes can be distributed systemically.

It is important to point out several features of this method that must be respected during model development. First, the optimal time for imaging after luciferase administration must be determined for each tumour line and implant location, which can easily be accomplished by collecting serial images as shown for the hollow fibres in Fig. 4. Secondly, it is important when using this approach for drug testing that drug treatment should be delayed until after the early tumour cell death has occurred (see Table 1) so that the tumours are in an actively growing phase during treatment. Thirdly, it seems apparent that cloning a transfected cell line to select for high expressors of luciferase would improve the detection limits. While this is true from the perspective of photons/s per cell, it is important to point out that selecting for a high producer of luciferase may select for a poorly tumorigenic cell line. If this happens, some improvement in the tumorigenicity may be achieved by re-isolating the tumour cells following serial *in vivo* passage.

One concern with this method was whether the administration of luciferin to the mice acts as a tumour-growth inhibitor. When we compared the growth of tumours exposed to luciferin to similar tumours that were not exposed there was no obvious tumour-inhibitory effect. Thus, repeated imaging of tumour-implanted mice is not expected to skew the growth data; however, this should be confirmed for each tumour used. With regard to luciferin administration, the possibility of a test compound interfering with luciferase activity must be considered when testing novel structures. *In vitro* testing should reveal any problems in this regard, but it is important to remember that *in vivo* metabolism could result in altered structures with potential impact on the enzyme activity.

The photons of light generated by luciferase activity within a tumour must pass through tissues to reach the detection system. In the course of this passage the photons are scattered and absorbed by the tissues [12]. This phenomenon is accentuated by the presence of tissue pigments and hair overlying the imaging field.

Therefore, applications of this technique in dark-skinned mice (e.g. C57Bl/6) results in reduced sensitivity compared to light-coloured mice. Furthermore, the presence of hair overlying the imaging region does dampen photon detection. For this reason, haired mice provide better imaging sensitivity if they are clipped before imaging.

The obvious limitation to using bioluminescence as an endpoint in efficacy studies is the requirement for tumour cell lines that express luciferase, either constitutively or under the control of inducible promoters. This problem is partly solved by the commercial availability of the luciferase gene in various formats that allow stable transfection of cell lines. Additionally, luciferase-expressing tumour cell lines, already characterised for *in vivo* utililty, are now available from Xenogen Corp. As more researchers begin to apply bioluminescence endpoints, further commercial sources are likely to become available.

In conclusion, we feel that bioluminescence provides an opportunity to create many new, clinically relevant efficacy models. These include a variety of models using orthotopic implant sites that were previously difficult to monitor for tumour growth. The use of bioluminescence may reduce the number of animals required for generating evidence of tumour growth inhibition, since it is more accurate that the classical techniques for tumour measurement. Improved sensitivities in detecting drug effects are available because small changes in tumour cell viability should be evident when luciferase is used as an endpoint rather than tumour mass. And finally, the availability of specific constructs, both as tumour lines and as transgenic mice, will allow dissection of *in vivo* drug effects in ways that were unavailable before.

References

1. Plowman J, Dykes DJ, Hollingshead M, Simpson-Herren L, Alley MC. Human tumor xenograft models in NCI drug development. In Teicher B, ed. *Anticancer Drug Development Guide: Preclinical Screening, Clinical Trials and Approval*. Totowa, NJ, Humana Press, 1997, 101–125.
2. Corey E, Quinn JE, Vessella RL. A novel method of generating prostate cancer metastases from orthotopic implants. *Prostate* 2003, **56**, 110–114.
3. te Velde EA, Vogten JM, Gebbink MF, van Gorp JM, Voest EE, Borel Rinkes IH. Enhanced antitumor efficacy by combining conventional chemotherapy with angiostatin or endostatin in a liver metastasis model. *Br J Surg* 2002, **89**, 1302–1309.
4. Contag CH, Jenkins D, Contag PR, Negrin RS. Use of reporter genes for optical measurements of neoplastic disease in vivo. *Neoplasia* 2000, **2**, 41–52.
5. Weissleder R, Ntziachristos V. Shedding light onto live molecular targets. *Tech Trends* 2003, **9**, 123–128.
6. Contag PR. Whole-animal cellular and molecular imaging to accelerate drug development. *DDT* 2002, **7**, 555–562.
7. Evelhoch JL, Gillies RJ, Karczmar GS, *et al*. Application of magnetic resonance in model systems: cancer therapeutics. *Neoplasia* 2000, **2**, 152–165.
8. Mahmood U, Weissleder R. Near-infrared optical imaging of proteases in cancer. *Mol Cancer Ther* 2003, **2**, 489–496.
9. Mankoff DA, Dehdashti F, Shields AF. Characterizing tumors using metabolic imaging: PET imaging of cellular proliferation and steroid receptors. *Neoplasia* 2000, **2**, 71–86.
10. Ntziachristos V, Bremer C, Weissleder R. Fluorescence imaging with near-infrared light: new technological advances that enable in vivo molecular imaging. *Eur Radiol* 2003, **13**, 195–208.
11. Paulus MJ, Gleason SS, Kennel SJ, Hunsicker PR, Johnson DK. High resolution X-rad computed tomography: an emergin tool for small animal cancer research. *Neoplasia* 2000, **2**, 62–70.
12. Rice BW, Cable MD, Nelson MB. In vivo imaging of light-emitting probes. *J Biomed Optics* 2001, **6**, 432–440.
13. Rudin M, Weissleder R. Molecular imaging in drug discovery and development. *Nat Reviews Drug Discovery* 2003, **2**, 123–131.
14. Bremer C, Ntziachristos V, Weissleder R. Optical-based molecular imaging: contrast agents and potential medical applications. *Eur Radiol* 2003, **13**, 231–243.
15. Bremer C, Mustafa M, Bogdanov Jr A, Ntziachristos V, Petrovsky A, Weissleder R. Stead-state blood volume measurements in experimental tumors with different angiogenic burdens a study in mice. *Radiology* 2003, **226**, 214–220.
16. Kim RY, Savellano MD, Weissleder R, Bogdanov Jr A. Steady-state and dynamic contrast MR imaging of human prostate cancer xenograft tumors: a comparative study. *Technol Cancer Res Treat* 2002, **1**, 489–495.
17. Kruger RA, Kiser WL, Reinecke DR, Kruger GA, Miller KD. Thermoacoustic molecular imaging of small animals. *Mol Imaging* 2003, **2**, 113–123.
18. Tai YC, Chatziioannou AF, Yang Y, *et al*. MicroPET II: design, development and initial performance of an improved microPET scanner for small-animal imaging. *Phys Med Biol* 2003, **48**, 1519–1537.
19. Cherry SR, Gambhir SS. Use of positron emission tomography in animal research. *ILAR J* 2001, **42**, 219–232.
20. Cherry SR. Fundamentals of positron emission tomography and application in preclinical drug development. *J Clin Pharmacol* 2001, **41**, 482–491.
21. Yang, H., Berger, F., Tran, C., Gambhir, S.S., Sawyers, C.L., MicroPET imaging of prostate cancer in LNCAP-SR39TK-GFP mouse xenografts. *Prostate* 2003, **55**, 39–47.
22. Hooper CE, Ansorge RE, Browne HM, Tomkins P. CCD imaging of luciferase gene expression in single mammalian cells. *J Biolumin Chemilumin* 1990, **5**, 123–130.
23. Bhaumik S, Gambhir SS. Optical imaging of Renilla luciferase reporter gene expression inliving mice. *Proc Natl Acad Sci USA* 2002, **99**, 377–382.
24. Bronstein I, Fortin J, Stanley PE, Stewart SAB, Kricka LJ. Chemiluminescent and bioluminescent reporter gene assays. *Analyt Biochem* 1994, **219**, 169–181.
25. Diehn FE, Costouros NG, Miller MS, *et al*. Noninvasive fluorescent imaging reliably estimates biomass in vivo. *BioTechniques* 2002, **33**, 1250–1255.
26. Burgos JS, Rosol M, Moats RA, Khankaldyyan V, Kohn DB, Nelson Jr MD, Laug WE. Time course of bioluminescent signal in orthotopic and heterotopic brain tumors in nude mice. *BioTechniques* 2003, **34**, 1184–1188.
27. Mahmood U, Tung C-H, Tang Y, Weissleder R. Feasibility of in vivo multichannel optical imaging of gene expression: experimental study in mice. *Radiology* 2002, **224**, 446–451.
28. Moon WK, Lin Y, O'Loughlin R, Tang Y, Kim D-E, Weissleder R, Tung C-H. Enhanced tumor detection using a folate receptor-targeted near-infrared fluorochrome conjugate. *Bioconjugate Chem* 2003, **14**, 539–545.

29. Petrovsky A, Schellenberger E, Josephson L, Weissleder R, Bodganov Jr A. Near-infrared fluorescent imaging of tumor apoptosis. *Cancer Res* 2003, **63**, 1936–1942.
30. Schellenberge EA, Bogdanov Jr A, Petrovsky A, Ntziachristos V, Weissleder R, Josephson L. Optical imaging of apoptosis as a biomarker of tumor response to chemotherapy. *Neoplasia* 2003, **5**, 187–192.
31. Graves EE, Ripoll J, Weissleder R, Ntziachristos V. A submillimeter resolution fluorescence molecular imging system for small animal imaging. *Med Phys* 2003, **30**, 901–911.
32. Wang JW, Yang M, Wang X, Sun FX, Li SM, Yagi S, Hoffman RM. Antimetastatic efficacy of oral 5-FU imaged by green fluorescent protein in real time. *Anticancer Res* 2003, **23**, 1–6.
33. Yamamoto N, Yang M, Jiang P, *et al. Clin Exp Metastasis* 2003, **20**, 181–185.
34. deWet JR, Wood KV, Jekinski DR, DeLuca M. Cloning of firefly luciferase cDNA and the expression of active luciferase in *Escherichia coli*. *Proc Natl Acad Sci USA* 1985, **82**, 7870–7873.
35. de Wet JR, Wood KV, DeLuca M, Helinski DR, Subramani S. Firefly luciferase gene: structure and expression in mammalian cells. *Mol Cell Biol* 1987, **7**, 725–737.
36. Contag CH, Spilman SD, Contag PR, *et al*. Visualizing gene expression in living mammals using a bioluminescent reporter. *Photochem Photobiol* 1997, **66**, 523–531.
37. Edinger M, Sweeney TJ, Tucker AA, Olomu AB, Negrin RS, Contag CH. Noninvasive assessment of tumor cell proliferation in animal models. *Neoplasia* 1999, **1**, 303–310.
38. Himmler A, Stratowa C, Czernilofsky AP. Functional testing of human dopamine D1 and D5 receptors expressed in stable camp-responsive luciferase reporter cell lines. *J Recept Res* 1993, **13**, 79–94.
39. Nguyen, J.T., Machado, H., Herschman, H.R., Repetitive, non-invasive imaging of cyclooxygenase-w gene expression in living mice. *Molec. Imaging Biol*., 2003, **5**, 248–256.
40. Pazzagli M, Devine JH, Peterson DO, Baldwin TO. Use of bacterial and firefly luciferases as reporter genes in DEAE-dextran-mediated transfection of mammalian cells. *Anal Biochem* 1992, **204**, 315–323.
41. Pons M, Gagne D, Nicolas JC, Mehtali M. A new cellular model of response to estrogens: a bioluminescent test to characterize (anti) estrogen molecules. *Biotechniques* 1990, **9**, 450–459.
42. Thompson JF, Hayes LS, Lloyd DB. Modluation of firefly luciferase stability and impact on studies of gene regulation. *Gene* 1991, **103**, 171–177.
43. Rapisarda A, Uranchimeg B, Scudiero DA, *et al*. Identification of small molecule inhibitors of hypoxia-inducible factor 1 transcriptional activation pathway. *Cancer Res* 2002, **62**, 4316–4324.
44. Hollingshead M, Plowman J, Alley M, Mayo J, Sausville. The hollow fiber assay. In Fiebig HH, Burger AM, eds. *Contributions to Oncology Vol 54: Relevance of Tumor Models for Anticancer Drug Development*. Basel, Karger, 1999, 109–120.